

Q^2 -evolution of the electric and magnetic polarizabilities of the proton

A. Sibirtsev and P. G. Blunden

Department of Physics and Astronomy, University of Manitoba, Winnipeg, MB, Canada R3T 2N2

The generalized Baldin sum rule at finite four-momentum transfer Q^2 is evaluated utilizing a structure function parameterization fit to recent experimental data. The most recent measurements on F_1 from Hall C at Jlab, as well as the F_2 structure function data from Hall B at Jlab and SLAC, were used in constructing our parameterization. We find that at Q^2 below 1 GeV² the dominant contribution to the electric and magnetic polarizabilities of the nucleon comes from the resonance region.

I. INTRODUCTION

Understanding the internal structure of strongly interacting particles is one of the major goals of low-energy QCD. The study of the response of baryons to an external electromagnetic field via the multipole excitation mechanism provides direct access to the internal structure.

The parameters to describe that response are electric, magnetic, and spin-dependent polarizabilities. The polarizability is an elementary structure constant that is related to the deformation and stiffness of the baryon. Furthermore, the physical content of the polarizabilities is an effective multipole interaction for the coupling of the electric and magnetic fields of the photon with the internal structure of the baryon [1, 2].

Evaluation of the electric (α) and magnetic (β) polarizabilities of the nucleon has attracted much attention, both phenomenological and theoretical. The Q^2 -dependence of the polarizabilities gives information on the polarization density in the nucleon. The Q^2 -evolution of the sum of both polarizabilities can be determined through the generalized Baldin sum rule [3], namely

$$\alpha(Q^2) + \beta(Q^2) = \frac{8\alpha_{\text{em}}M}{Q^4} \int_0^{x_\pi} x F_1(x, Q^2) dx, \quad (1)$$

where Q^2 is four-momentum transfer squared, α_{em} is the fine structure constant, M stands for the nucleon mass, and F_1 is the nucleon structure function. Here x is the Bjorken scaling variable,

$$x = \frac{Q^2}{W^2 - M^2 + Q^2}, \quad (2)$$

where W is the invariant mass of the final state, and x_π corresponds to pion threshold. This implies that F_1 should be taken up to an infinite energy. Indeed it is necessary to use quite reliable models for the W -dependence as well as Q^2 -dependence of the structure function in order to reduce the uncertainty of the sum rule evaluation.

Equation (1) provides information about the Q^2 -evolution of the polarizabilities. An evaluation of the Q^2 -dependence of the sum of electric and magnetic polarizabilities was done in 2006 by Liang *et al.* [4]. There was not much data on the F_1 structure function in the relevant kinematic region at that time. At high energies

the SLAC Rosenbluth data [5] were used. In the resonance region the E94-110 measurements [6, 7] in Hall C at Jefferson Laboratory (JLab) from 2004 were used.

Up to now this evaluation of the Q^2 -dependence of polarizabilities stands as the present “state of the art”. However, in 2013 an updated version of the E94-110 measurement appeared [8]. This has motivated us to reexamine the generalized Baldin sum rule.

At $Q^2 = 0$ the sum of electric and magnetic polarizabilities of the nucleon can be related to the unpolarized photo-absorption cross section $\sigma_{\gamma N \rightarrow X}$ as

$$\alpha + \beta = \frac{1}{2\pi^2} \int_{\nu_\pi}^{\infty} \frac{\sigma_{\gamma N \rightarrow X}(\nu)}{\nu^2} d\nu, \quad (3)$$

where ν is the photon energy and ν_π is pion photo-production threshold. It is clear that at $Q^2 = 0$ Eq. (1) converges to Eq. (3), since

$$x = \frac{Q^2}{2M\nu}. \quad (4)$$

Indeed, Eq. (3) is the original formulation of the Baldin sum rule [9, 10].

The evaluation of the Baldin sum rule requires knowledge of the energy-dependence of $\sigma_{\gamma N \rightarrow X}(\nu)$ up to $\nu \rightarrow \infty$. However, as the integral is weighted by $1/\nu^2$, the contribution at low energies dominates the integral.

The sum of the polarizabilities for the proton was evaluated by Damashek and Gilman [11] in 1970, and amounts to

$$\alpha + \beta = (14.2 \pm 0.3) \times 10^{-4} \text{ fm}^3. \quad (5)$$

A more recent calculation of Eq. (3) was done by Babusci *et al.* [12], with the result

$$\alpha + \beta = (13.69 \pm 0.14) \times 10^{-4} \text{ fm}^3. \quad (6)$$

The current PDG [13] averaged experimental values for electric and magnetic polarizabilities for proton are

$$\alpha = (12.0 \pm 0.6) \times 10^{-4} \text{ fm}^3, \quad (7a)$$

$$\beta = (1.9 \pm 0.5) \times 10^{-4} \text{ fm}^3. \quad (7b)$$

Finally, a Chiral Perturbation Theory calculation [14] predicts

$$\alpha + \beta = (14.0 \pm 4.1) \times 10^{-4} \text{ fm}^3 \quad (8)$$

for the proton. An evaluation of the generalized polarizabilities at low Q^2 was considered by Hemmert *et al.* [15].

A review of nucleon polarizabilities at $Q^2 = 0$ extracted from experimental data, as well as given by theoretical calculation, can be found in Ref. [1]. A more recent review within the effective field theory approach can be found in Ref. [16]. The polarizabilities at $Q^2 = 0$ provide a lower limit for the Q^2 -dependence of the generalized Baldin sum rule.

Here we calculate the generalized Baldin sum rule, aiming to obtain the Q^2 -dependence of the sum of generalized electric and magnetic proton polarizabilities. As a corollary, we obtain a convenient parameterization of the F_1 structure function from recent experimental data which is valid in the low- Q^2 , low W kinematic region.

The most recent results [8] for the F_1 structure function measured at Jlab Hall C were used for the contribution in the resonance region. Furthermore, we adopted the results on the F_2 structure function in the resonance region obtained at JLab. For that we apply the relation between F_2 and F_1 given by the ratio of longitudinal to transverse cross sections. That procedure provides us reasonable confidence in constructing the parameterization of the structure functions.

At energies above the resonance region we adopt the Regge approach. It is shown here that the Regge results are in good agreement with MRST leading twist fit [17, 18] at $Q^2 > 1 \text{ GeV}^2$. Note that the MRST parton distribution function is not provided for $Q^2 < 1 \text{ GeV}^2$.

The paper is organized as follows. In Sec. II we show the details of our parameterization of the structure functions, and compare it with experimental results. The evaluation of the generalized Baldin sum rules is given in Sec. III. The paper ends with a summary.

II. THE PARAMETERIZATION

For the F_1 structure function we use the parameterization developed in Ref. [19]. The parameters of that model were obtained from the fit of experimental results for the F_2 structure function measured at JLab [7, 20–22], as well as obtained at SLAC [23]. The structure functions F_1 and F_2 are related through the ratio of the longitudinal σ_L to transverse σ_T virtual photon cross sections as

$$R = \frac{\sigma_L}{\sigma_T} = \frac{F_2}{2xF_1} \left[1 + \frac{4M^2x^2}{Q^2} \right] - 1. \quad (9)$$

Figure 1 shows the experimental results for the ratio. The circles indicate the data [8] from Jlab Hall C, while the squares are the data from SLAC [5]. The ratio is shown for different Q^2 . Here solid lines are our parameterization, given as

$$R = 0.014 Q^2 \left[\exp(-0.07 Q^2) + 41 \exp(-0.8 Q^2) \right], \quad (10)$$

with Q^2 in units of GeV^2 .

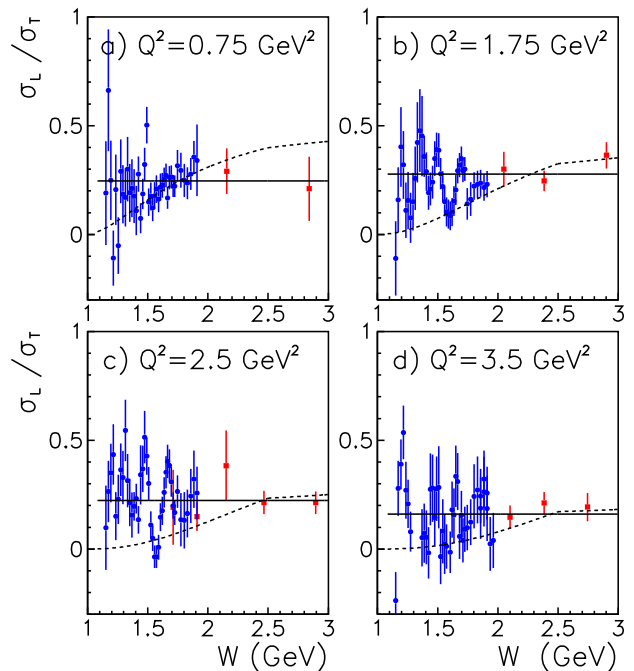


FIG. 1: (Color online). The ratio of the longitudinal σ_L to transverse σ_T virtual photon cross sections as a function of energy W shown for different Q^2 . The circles are the results [8] from Jlab Hall C. The squares are the results from SLAC [5]. Solid lines are our parameterization given by Eq. (10). Dashed lines show the parameterization from Ref. [24].

Actually the parameters of Eq. (10) were obtained from a fit of the experimental results shown in Fig. 1. Since the data at $W < 2 \text{ GeV}$ are given with quite large statistical and experimental errors, we were not able to fit the fine structure of the ratio in the resonance region. Equation (10) provides a correct limit at $Q^2 = 0$ (*i.e.* $R = 0$), since at the real photon point $\sigma_L = 0$. Equation (10) was used to obtain the parameterization for the F_1 structure function from that given [19] for F_2 .

Now we give the details of the F_2 parameterization, since these were not published in Ref. [19]. We did consider two regions with respect to energy W , namely the resonance and DIS regions.

At $W < 1.9 \text{ GeV}$ we use the isobar model following the analyses of Refs. [25–27]. The contributions from four resonances, namely $P33(1232)$, $D13(1520)$, $F15(1680)$ and $F37(1950)$, were considered. The resonance properties adopted in our analysis are listed in Table I. Note that the masses and widths of the resonances were not taken from PDG [13], but were obtained from the fit of experimental results for the F_2 structure function.

The resonance construction was parameterized by a relativistic Breit-Wigner shape as

$$\sigma_R = \frac{A_R M_R^2 \Gamma_1 \Gamma_2 G(Q^2)}{(M_R^2 - W^2)^2 + M_R^2 \Gamma_1^2} \left(\frac{k_R}{k} \right)^2, \quad (11)$$

and we account for the energy-dependence of the width,

namely

$$\Gamma_1 = \Gamma_R \left(\frac{q}{q_R} \right)^{2l+1} \left(\frac{q^2 + x_R^2}{q_R^2 + x_R^2} \right)^l, \quad (12a)$$

$$\Gamma_2 = \Gamma_R \left(\frac{q}{q_R} \right)^{2l} \left(\frac{k^2 + x_R^2}{k_R^2 + x_R^2} \right)^l. \quad (12b)$$

Furthermore

$$k = \frac{\lambda^{1/2}(W^2, m_N^2, Q^2)}{2W}, \quad (13a)$$

$$k_R = \frac{\lambda^{1/2}(M_R^2, m_N^2, Q^2)}{2M_R}, \quad (13b)$$

$$q = \frac{\lambda^{1/2}(W^2, m_N^2, m_\pi^2)}{2W}, \quad (13c)$$

$$q_R = \frac{\lambda^{1/2}(M_R^2, m_N^2, m_\pi^2)}{2M_R}, \quad (13d)$$

with the kinematical function λ defined as

$$\lambda(x, y, z) = (x - y - z)^2 - 4yz. \quad (14)$$

We introduce form factors at the interaction vertices, parameterized by an overall exponential function as

$$G(Q^2) = \exp(-bQ^2), \quad (15)$$

with cut off parameters b listed in Table 1. The parameters were fit to data [19] on the F_2 -structure function.

With respect to Ref. [28], we do not consider $S11(1535)$, $S11(1650)$, and $P11(1440)$ resonances. We found that it is difficult to separate these resonances from others in performing the fit and keep the resonance properties (*e.g.* strength, width) as free parameters. Since our strategy was to describe the experimental results on the structure function, not to study baryons, this approach seems quite reasonable.

Moreover, in the resonance region we consider in addition the non-resonant background contribution F_2^{bg} . It was parameterized as

$$F_2^{\text{bg}} = c_1 c_2 \frac{(1-x)^{1.5}}{x^{0.6}}, \quad (16a)$$

$$c_1 = 4\pi^2 \alpha_{\text{em}} \frac{Q^2 + a_\nu^2}{Q^2 a_\nu^2 (1-x)}, \quad (16b)$$

$$c_2 = 0.0037575 + 0.075834 Q^2 + 0.024600 Q^4 - 0.0099514 Q^6, \quad (16c)$$

$$x = \frac{Q^2}{2(M + m_\pi)a_\nu}, \quad (16d)$$

$$a_\nu = \frac{W^2 + Q^2 - (M + m_\pi)^2}{2(M + m_\pi)}. \quad (16e)$$

TABLE I: Resonance parameters used in our isobar model.

Res.	M_R (GeV)	Γ_R (GeV)	l	x_R	b (GeV $^{-2}$)	A_R
$P33$	1.22	0.119	1	0.16	1.51	723.1
$D13$	1.52	0.127	2	0.35	1.32	214.6
$F15$	1.70	0.117	3	0.35	0.81	95.6
$F37$	1.90	0.28	3	0.35	1.11	68.2

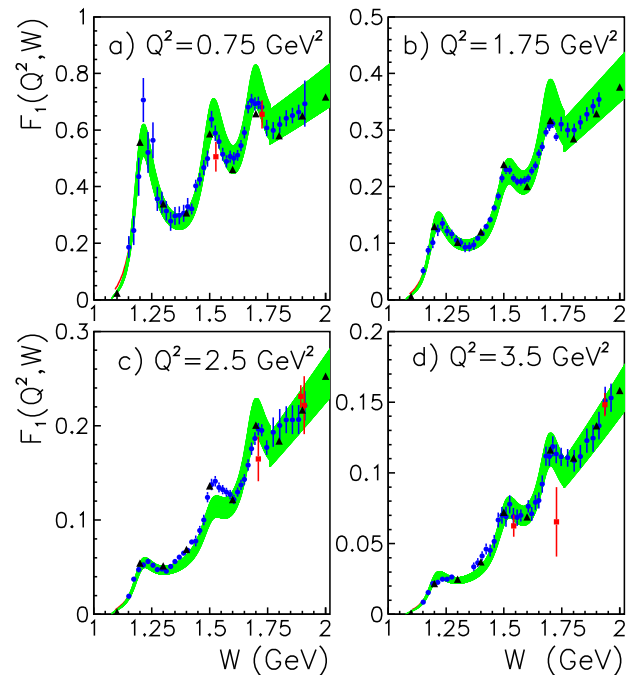


FIG. 2: (Color online). F_1 structure function in the resonance region ($W < 2$ GeV) shown for different Q^2 values. The circles are the results [8] from JLab Hall C, while the squares are from SLAC [5]. The shaded (green) band represents the uncertainty on our fit. The triangles are the results from the parameterization given in Ref. [28].

Figure 2 shows our calculations together with data for the F_1 structure function. The circles are experimental results from JLab [8], and the squares indicate data from SLAC [5]. The shaded band represents the uncertainty in our fit. The triangles are results from the parameterization in Ref. [28]. It is clear that both parameterizations describe the data quite reasonably, although they are constructed in a different manner.

Above the resonance region we adopt the Regge model [29–31]. The advantage of the Regge approach is that it can be used as well at low Q^2 , where the MRST PDF description cannot be applied. The comparison of Regge results with MRST and data is given in Fig. 3. There is a reasonable agreement between MRST and Regge results, as well as describing the available data.

III. POLARIZABILITIES

Now with the given parameterization for the F_1 structure function, we calculate the sum of electric and magnetic polarizabilities of the proton. Since the parameters of the model were fitted at $Q^2 > 0.225$ GeV 2 , the results shown in Fig. 4 are for the relevant region. Here the dashed line indicates the result for energies $W < 2$ GeV. The solid line is the result for the full range of energy. The square illustrates the prediction [14] from ChPT.

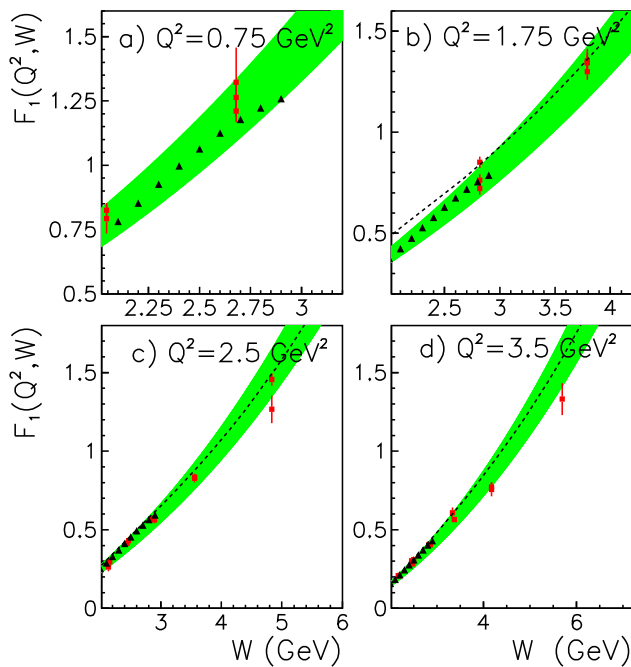


FIG. 3: (Color online). F_1 structure function above the resonance region shown for different Q^2 values. The squares are from SLAC [5]. The shaded (green) band represents the uncertainty on our fit. The triangles are the results from the parameterization given in Ref. [28]. The dashed lines illustrate results from MRST [17, 18].

We also show recent experimental results from Hall A given at $Q^2 = 0.92 \text{ GeV}^2$ and 1.76 GeV^2 and evaluated by the dispersion relation approach. Unfortunately statistical and systematic errors of the data are too large, so it is not possible to make solid conclusions on the compatibility of our analysis and measurements. It appears that further precise experiments are required. Furthermore, at $Q^2 < 1 \text{ GeV}^2$ the dominant contribution to polarizabilities comes from the resonance region.

IV. SUMMARY

We evaluated the generalized Baldin sum rule using a structure function parameterization fit to experimental data. The most recent data on F_1 from Hall C at JLab were used in our analysis. As well, we utilized the F_2 structure function data collected by the Hall B Collaboration at JLab and the F_2/F_1 ratio. SLAC results are also included in our analysis. We found that

at $Q^2 < 1 \text{ GeV}^2$ the dominant contribution to the sum of electric and magnetic polarizabilities comes from the resonance region, *i.e.* at energies $W < 2 \text{ GeV}$.

Further study is necessary at $Q^2 < 0.2 \text{ GeV}^2$ to establish the transition to the real photon point. In the absence of experimental results in that region we could not develop a phenomenological model. It is important

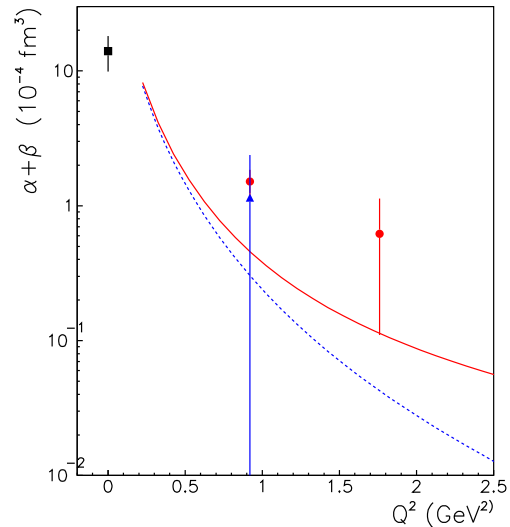


FIG. 4: (Color online). The sum of the electric and magnetic polarizabilities of the proton as a function of Q^2 . The dashed line indicates the result for $W < 2 \text{ GeV}$, while the solid line shows our calculation for the full range of energy. The square is the prediction [14] given by Chiral Perturbation Theory at $Q^2 = 0$. Circles are the results from Hall A obtained with a dispersion relation approach and using data sets I-a and II [32]. The triangle result is for data set I-b.

to construct a reliable parameterization for F_1 structure function if possible. We keep this study in progress.

We note that linear extrapolation of our results to the real photon point does not allow us to get polarizability at $Q^2 = 0$. That issue as well requires a more detailed study at low Q^2 .

Acknowledgments

We would like to thank M.E. Christy and P.E. Bosted for providing us with their code, and V. Tvaskis, E. Epelbaum, and Ulf-G. Meißner for many useful discussions.

[1] D. Babusci *et al.*, Phys. Rev. **C58**, 1013 (1998).
 [2] B. R. Holstein, D. Drechsel, B. Pasquini, and M. Vanderhaeghen, Phys. Rev. **C61**, 034316 (2000).

[3] D. Drechsel, B. Pasquini, and M. Vanderhaeghen, Phys. Rep. **378**, 99 (2003).
 [4] Y. Liang, M.E. Christy, R. Ent, and C.E. Keppel, Phys.

- Rev. **C73**, 065201 (2006).
- [5] L. W. Whitlow *et al.*, Phys. Lett. B **250**, 193 (1990).
- [6] Y. Liang, Ph.D. thesis, The American University, 2003
- [7] Y. Liang *et al.*, arXiv:nucl-ex/0410027v1, 2004.
- [8] Y. Liang *et al.*, arXiv:nucl-ex/0410027v2, 2013.
- [9] A. M. Baldin, Nucl. Phys. **18**, 310 (1960).
- [10] L. I. Lapidus, Sov. Phys. JETP **16**, 964 (1963)
- [11] M. Damashek and F. J. Gilman, Phys. Rev. **D1**, 1319 (1970).
- [12] D. Babusci, G. Giordano, and G. Matone, Phys. Rev. **C57**, 291 (1998).
- [13] J. Beringer *et al.* (Particle Data Group), Phys. Rev. **D86**, 010001 (2012).
- [14] V. Bernard, N. Kaiser, and Ulf-G. Meißner, Int. J. Mod. Phys, **E4**, 193 (1995).
- [15] T. R. Hemmert, *et al.*, Phys. Rev. Lett. **79**, 22 (1997); Phys. Rev. D **62**, 014013 (2000).
- [16] H. W. Griesshammer, J. A. McGovern, D. R. Phillips, and G. Feldman, Prog. Part. Nucl. Phys. **67**, 841 (2012).
- [17] A. D. Martin, R. G. Roberts, W. J. Stirling, and R. S. Thorne, Eur. Phys. J. **C28**, 455 (2003).
- [18] A. D. Martin, W. J. Stirling, R. S. Thorne, and G. Watt, Phys. Lett. B **652**, 292 (2007).
- [19] A. Sibirtsev, P. G. Blunden, W. Melnitchouk, and A. W. Thomas, Phys. Rev. **D82**, 013011 (2010).
- [20] M. Osipenko *et al.*, Phys. Rev. **D67**, 092001 (2003).
- [21] I. Niculescu *et al.*, Phys. Rev. Lett. **85**, 1186 (2000).
- [22] S. P. Malace *et al.*, Phys. Rev. **C80**, 035207 (2009).
- [23] L. W. Whitlow *et al.*, Phys. Lett. B **282**, 475 (1992).
- [24] G. Ricco *et al.*, Nucl. Phys. **B555**, 306 (1999).
- [25] A. A. Cone *et al.*, Phys. Rev. **156**, 1490 (1967).
- [26] S. Stein *et al.*, Phys. Rev. **D12**, 1884 (1975).
- [27] F. W. Brasse *et al.*, Nucl. Phys. **B110**, 413 (1976).
- [28] M.E. Christy and P.E. Bosted, Phys. Rev. C **81**, 055213 (2010).
- [29] A. Capella, A. Kaidalov, C. Merino and J. Tran Thanh Van, Phys. Lett. B **337**, 358 (1994).
- [30] A. B. Kaidalov and C. Merino, Eur. Phys. J. C **10**, 153 (1999).
- [31] H. Abramowicz, E. M. Levin, A. Levy and U. Maor, Phys. Lett. B **269**, 465 (1991).
- [32] H. Fonvieille *et al.*, Phys. Rev. C **86**, 015210 (2012).